Cerebral Cortex, March 2020;30: 875–887

doi: 10.1093/cercor/bhz133
Advance Access Publication Date: 29 July 2019
Original Article

ORIGINAL ARTICLE

The Human Intraparietal Sulcus Modulates Task-Evoked Functional Connectivity

Kai Hwang[1,2,*], James M. Shine[3,4], Dillan Cellier[1,2] and Mark D'Esposito[1]

[1]Helen Wills Neuroscience Institute and Department of Psychology, University of California, Berkeley, CA, USA, [2]Department of Psychological and Brain Sciences and the Iowa Neuroscience Institute, The University of Iowa, Iowa, IA, USA, [3]Department of Psychology, Stanford University, Palo Alto, CA, USA and [4]Brain and Mind Centre, The University of Sydney, Sydney, NSW, Australia

Address correspondence to Kai Hwang, Department of Psychological and Brain Sciences—W300 SSH 301 E. Jefferson St Iowa City, IA 52245, USA. Email: kai-hwang@uiowa.edu http://orcid.org/0000-0002-1064-7815

Abstract

Past studies have demonstrated that flexible interactions between brain regions support a wide range of goal-directed behaviors. However, the neural mechanisms that underlie adaptive communication between brain regions are not well understood. In this study, we combined theta-burst transcranial magnetic stimulation (TMS) and functional magnetic resonance imaging to investigate the sources of top-down biasing signals that influence task-evoked functional connectivity. Subjects viewed sequences of images of faces and buildings and were required to detect repetitions (2-back vs. 1-back) of the attended stimuli category (faces or buildings). We found that functional connectivity between ventral temporal cortex and the primary visual cortex (VC) increased during processing of task-relevant stimuli, especially during higher memory loads. Furthermore, the strength of functional connectivity was greater for correct trials. Increases in task-evoked functional connectivity strength were correlated with increases in activity in multiple frontal, parietal, and subcortical (caudate and thalamus) regions. Finally, we found that TMS to superior intraparietal sulcus (IPS), but not to primary somatosensory cortex, decreased task-specific modulation in connectivity patterns between the primary VC and the parahippocampal place area. These findings demonstrate that the human IPS is a source of top-down biasing signals that modulate task-evoked functional connectivity among task-relevant cortical regions.

Key words: intraparietal sulcus, cognitive control, functional connectivity, TMS, working memory

Introduction

In our daily lives, we constantly face situations where we need to flexibly regulate thoughts and actions in response to changing goals. Previous studies suggest that neural systems implement top-down control by exerting biasing signals to adaptively modulate on-going perceptual, motor, and cognitive functions (Miller and Cohen 2001; D'Esposito and Postle 2015). In support of this notion, studies have shown that top-down biasing signals can adaptively modulate the response amplitude of localized brain activity (O'Craven et al. 1999; Druzgal and D'Esposito 2001), resulting in both enhancement of responses to task-relevant stimuli and suppression of responses to task-irrelevant stimuli (Gazzaley et al. 2005). These biasing signals can also modulate spatial patterns of activity within local functional brain regions (Seidl et al. 2012; Nelissen et al. 2013). For example, goal-directed attention influences the decoding accuracy of multi-voxel patterns of activity in occipito-temporal cortices (Chen et al. 2012) and their tuning to attended stimuli (Serences et al. 2009).

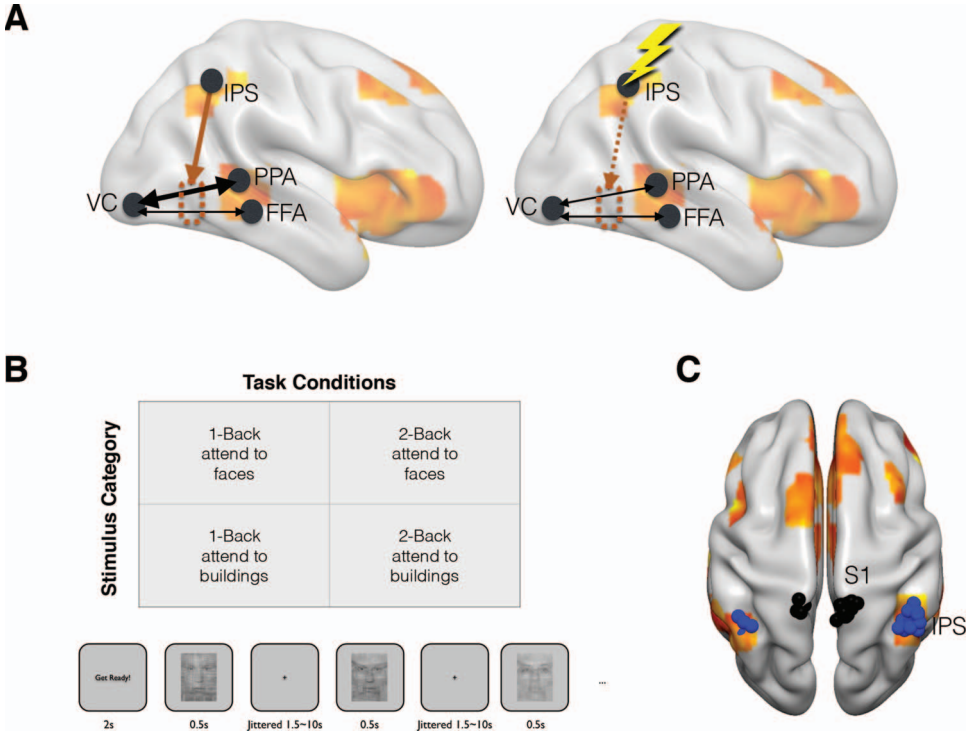

Figure 1. (A) We hypothesized that functional connectivity between VC and FFA/ PPA will be modulated by attention and memory load. For example, when attending to buildings during the task, there should be an increase in functional connectivity between VC and PPA (left). Following disruption of IPS function with TMS, there should be a decrease in task-evoked modulation in functional connectivity between these regions (right). (B) Structure of the task and trial timing (C) Individual subject TMS target sites: IPS (blue spheres) and S1 (black spheres) stimulation sites. Yellow/orange areas represent regions that exhibit increased correlation with task-evoked changes in connectivity between VC and FFA/PPA across all task conditions.

Neural systems exert top-down control not only by modulating localized information representation, but also through modulation of interactive communication between distributed brain regions (Van Essen et al. 1992; Friston 2009). For example, while attending to a visual object, information related to elementary visual features encoded in the primary visual cortex (VC) is transmitted to anterior ventral temporal cortices for further processing (Lerner et al. 2001). These findings suggest that top-down control could also be achieved by adaptively regulating the information flow between brain regions to prioritize the transfer of task-relevant information (Botvinick et al. 2001). Functional interactions that reflect information transfer between brain regions can be estimated by calculating the statistical dependency between activity in different brain regions, otherwise known as functional connectivity.

In our previous study (Hwang et al. 2019), we investigated the potential sources of top-down biasing signals that modulate task-evoked functional connectivity patterns by searching for brain regions that covary with changes in functional connectivity strength. We found that task-evoked changes in functional connectivity strength interacted with localized activity in frontal and parietal cortices, suggesting that frontal and parietal cortices could modulate information communication between brain regions. However, these results provided only correlational evidence for this hypothesis; it is possible that these regions did not actively influence connectivity patterns, but rather receive information from other brain regions. Furthermore, our previous study utilized a block design, making it difficult to isolate error trials and probe the relationship between functional connectivity strength and behavioral performance. Thus, the behavioral significance of task-evoked functional connectivity we previously observed also remains unclear.

To address these issues, the current study utilized a causal method, continuous theta-burst transcranial magnetic stimulation (tb-TMS), combined with functional magnetic resonance imaging (fMRI), to test the role of the superior intraparietal sulcus (IPS) in modulating task-evoked functional connectivity. The IPS showed the greatest effect in our previous study, and other previous studies have proposed that the IPS could adaptively gate information transfer between visual regions for selective attention (Friston and Buschel 2000; Stephan et al. 2008). Thus, we administered tb-TMS to the IPS and to a control region, the medial primary somatosensory area (S1), prior to fMRI scanning. During scanning, subjects performed an n-back task comprised of visual stimuli drawn from two categories (faces and buildings), each of which is known to engage a different ventral temporal region (e.g., faces for fusiform face area [FFA], and buildings for parahippocampal place area [PPA]). We utilized a mixed-block event related design that allowed us to separately analyze correct versus incorrect trials (Visscher et al. 2003), and tested two hypotheses in this study. First, task-specific modulation of functional connectivity strength between brain regions that process task-relevant information can be modulated by memory load and stimuli relevancy. Second, IPS is a source of top-down biasing signals that modulate functional connectivity between brain regions, in which case disruption of IPS function with TMS should decrease task-specific modulation of functional connectivity (Fig. 1A).

Methods

Subjects

Twenty-seven healthy adult subjects were recruited for this study. Two subjects were excluded because of a hardware issue, and two subjects were excluded because of drowsiness or poor task compliance in the MRI scanner. Therefore, baseline fMRI analyses were performed on 23 subjects (aged 18–35, nine males). Analyses of the TMS data were limited to the 17 subjects who completed all TMS testing sessions. All subjects were right handed, had normal or corrected-to-normal vision, and reported no history of a neurological or psychiatric disorder. All subjects provided written informed consent in accordance with procedures approved by the Committee for the Protection of Human Subjects at the University of California, Berkeley.

Experimental Design

A within-subject design was used to test the effects of TMS on brain function. Subjects first completed a baseline fMRI session, followed by two TMS-fMRI sessions. During the baseline session, subjects' fMRI data were used to identify regions of interests (ROI) for further analyses and to localize subject-specific ROIs for tb-TMS. During the two TMS-fMRI testing sessions, subjects received tb-TMS to either the IPS or S1, and the order of stimulation sites was randomized across subjects. The fMRI data were collected within 10 min after tb-TMS to either IPS or S1 to assess TMS effects.

Data Acquisition

Imaging data were acquired using a Siemens Tim/Trio 3T scanner and a 32-channel head coil located at the Henry H. Wheeler Jr Brain Imaging Center at the University of California, Berkeley. Structural images were acquired using a multi-echo MPRAGE sequence (TR = 2530 ms; TE = 1.64/3.5/5.36/7.22 ms; flip angle = 7°; field of view = 256 x 256, 176 sagittal slices, 1 mm^3 voxels; 2x GRAPPA acceleration). Functional images were acquired using an echo-planar sequence sensitive to blood oxygenated level-dependent (BOLD) contrast with multiband acceleration (TR = 1000 ms; TE = 33.2 ms; flip angle = 40°; voxel size: 2.5 mm^3 isotropic voxels with 52 axial slices; multiband factor = 4). The first five subjects in this study completed 18 runs of functional scans for the baseline fMRI session and 12 runs for the TMS-fMRI sessions, with each run lasting 2 min and 35 s (155 TRs per run). The next 18 subjects completed 12 runs of functional scans during the baseline fMRI session and eight runs during the TMS-fMRI session, with each run lasting 3 min and 56 s (236 TRs per run). The change in run length was made to reduce start-up time between task runs and to keep the total session run time under the allocated time limit. Despite the differences in run structure, the total number of trials administered per condition were identical (78 trials per condition), and total fMRI volumes collected per condition were comparable between subjects (465 vs. 472 volumes). An LCD projector projected visual stimuli onto a screen mounted to the MRI gradient head coil. Psychophysics Toolbox Version 3 was used to present stimuli and record responses via a fiber-optic motor response recording device.

Experimental Tasks

During all fMRI sessions, subjects performed tasks that required them to respond to sequentially presented pictures randomly drawn from a set of 120 pictures of human faces and buildings. Specifically, subjects completed a functional localizer task, a 1-back task, and a 2-back task (Fig. 1B). The functional localizer task was used to localize the FFA (Kanwisher et al. 1997) and the PPA (Epstein et al. 1999). In this task, pictures of human faces or buildings were presented briefly to subjects, who were required to make a button press to identify the category of the picture presented (face or building). For the n-back tasks, two factors were manipulated: memory load (2-back vs. 1-back) and the stimuli relevance (attend faces vs. attend buildings). Images presented in the 1-back and 2-back tasks were pictures of semi-transparent faces overlapped with semitransparent buildings (see Fig. 1B). Luminance for all pictures was equalized using the SHINE toolbox (Willenbockel et al. 2010). Feedback was given at the end of each run indicating the accuracy of responses.

Prior to the start of each task, subjects were instructed to attend to a target category (faces or buildings), and to detect the occasional stimulus repetition of the attended target category. For the 2-back task, subjects were required to decide if the current picture presented matched the picture presented two trials back, whereas for the 1-back task subjects decided whether the current picture matched the picture in the previous trial. On different runs, subjects used their left or right index finger to respond. The response-mapping was randomized, balanced across tasks and runs, and explicitly instructed to the subjects before the start of each functional run.

Each fMRI run contained only one task condition, and subjects were visually presented with detailed task instructions prior to the start of each run. All runs began with 3 s of initial fixation, followed by task blocks interleaved with baseline fixation blocks. For the five subjects who performed tasks with shorter runs (155 s), each run consisted of two 60-second task blocks interleaved with 25 s of rest block and 7 s of a final fixation. For the rest of the subjects, each run consisted of three 60-second task blocks interleaved with two 30-second rest blocks and a 10-second final fixation. For all subjects, each task block started with a 2-second initiation cue, followed by 13 trials of stimuli. Each trial started with an image presented centrally on screen for 500 ms, immediately followed by a randomly jittered intertrial fixation that lasted between 1.5 to 10 s, sampled from an exponential distribution. Within each block, there were two to four repetitions of both stimuli categories, with the presentation sequences randomized separately. For all participants, 78 trials were administered for each condition.

fMRI Data Preprocessing

Imaging data were preprocessed using FMRIPREP version 1.0 (Esteban et al. 2018). Each T1 anatomical image was corrected for intensity nonuniformity and skull-stripped using ANTS v2.1.0 (Avants et al. 2011). Brain surfaces were reconstructed using Freesurfer (Dale et al. 1999; Fischl et al. 1999). Anatomical scans were then normalized to the ICBM 152 Nonlinear Asymmetric template version 2009c through nonlinear registration using ANTS. Functional data were motion-corrected using FSL's MCFLIRT, and registered to the anatomical T1 image using a boundary-based registration with nine degrees of freedom. Motion correction and BOLD-to-T1 transformations were concatenated and applied in a single-step interpolation. Preprocessed data in native space, without normalization to the Montreal Neurological Institute (MNI) Template space, were also saved. Functional data were then spatially smoothed with a 4 mm full-width-at-half-maximum Gaussian kernel (FSL's

SUSAN). A nuisance regression was then performed using ordinary least squares regression (AFNI's 3dDeconvolve) with the following regressors: polynomial fits for removing linear drifts, six rigid-body motion parameters and their derivatives, and averaged signal from white-matter and ventricle ROIs that were created using Freesurfer's tissue segmentation tool (Dale et al. 1999). To minimize motion confounds, framewise displacement (FD) was calculated and volumes with FD > 0.2 were removed prior to all regression analyses to reduce variances associated with high-noise timepoints.

fMRI ROI

ROIs were defined using methods previously reported in Hwang et al. 2019. To estimate the evoked response associated with each trial, a voxel-wise generalized least squares regression with ARMA(1,1) autocorrelation model (AFNI's 3dREMLfit) was performed. Finite impulse response (FIR) basis functions were used to estimate the mean stimulus-evoked response amplitudes associated with each condition. Specifically, for each trial type a total of 14 FIR regressors were used to model 14 s of trial-locked hemodynamic response after stimulus onset. Correct and incorrect trials were modeled separately, and only correct trials were included into evoked amplitude analyses. The estimated response magnitude 3 to 9 s after the stimulus onset was then averaged. We defined the FFA using the top 255 voxels (size equivalent to a sphere with 8 mm radius) within the previously defined FFA ROIs (Julian et al. 2012) that exhibited the strongest evoked response for faces compared to buildings. We repeated this procedure for definition of the PPA, except with buildings compared to faces (building blocks > faces blocks), and only for voxels within previously defined PPA ROIs (Julian et al. 2012). For all subjects, the primary VC ROI was defined using the top 255 most active voxels within the anatomical ROI along the calcarine sulcus from Freesurfer (Destrieux et al., 2010). We did not use a conventional spherical ROI centering around peak coordinates in the interest of avoiding including nongray matter voxels.

To localize potential sources of top-down biasing signals that modulate task-evoked functional connectivity, we combined a time-varying functional connectivity analysis with whole-brain regression. Prior to preforming all connectivity analyses, variances associated with the averaged stimulus-evoked responses patterns, as estimated by FIR models (see above), were removed from the data via linear regression (Cole et al. 2018). This procedure removes the mean stimuli-evoked response patterns from the data while preserving the trial-by-trial task variance for connectivity calculations. It has been shown that FIR task regression is most effective in reducing false positives in connectivity estimates when analyzing task fMRI data (Cole et al. 2018). This procedure controls for the confound of spurious increases in functional connectivity by correlated increases in stimulus-evoked response amplitudes within the overlapping receptive fields between VC/FFA/PPA.

Time varying connectivity strength between early visual areas and PPA/FFA was then estimated under different task conditions using the Multiplication of Temporal Derivatives method (MTD) (Shine et al. 2015). Briefly, the first-order temporal derivatives (dt) of each time series were first calculated, and then normalized to each data point by dividing each derivative by the standard deviation of the whole time-series. The dt scores were then multiplied to calculate MTD scores between ROIs. Positive MTD scores indicate strong coupling between ROIs, whereas negative MTD scores reflect decoupling. MTD scores can then be averaged across time to derive an estimate akin to static functional connectivity strength, whereas the time-varying MTD scores that are not averaged reflect time-varying changes in the strength of functional connectivity between ROIs. Individual MTD scores corresponding to each stimulus onset can also be extracted to derive estimates of trial-by-trial fluctuations in functional connectivity strength.

Because MTD scores could be susceptible to high frequency noise, it is necessary to calculate a moving average on MTD scores. Thus, we performed simulations of different window lengths to estimate the sensitivity for detecting task-evoked changes in connectivity across various window sizes (see Hwang et al. 2019 for details). We found that a window size of 15 volumes results in maximum sensitivity—the same window size used in our previous study that demonstrated that task-related effects in MTD estimates were stable across a range of moving windows from 5 to 15 (Hwang et al. 2019). Therefore, all results are presented using this window size. In our previous study, we found that results from MTD analyses were consistent with results calculated using the more conventional Pearson correlation coefficient. Specifically, we found that the direction of task differences between conditions were consistent between Pearson correlations and MTD estimates. For consistency, and because MTD has the advantage of providing a time-varying regressor for whole-brain regression analysis, we performed all connectivity analyses using MTD.

TMS ROIs

MTD time-series for each condition were used as regressors in a general linear model (GLM) analysis to localize regions that covary with time-varying changes in functional connectivity strength. Using a similar procedure, we previously found that the bilateral, superior IPS exhibited the strongest association with time-varying changes in functional connectivity strength (Hwang et al. 2019). Therefore, for each subject, we performed whole-brain GLM analysis using MTD regressors, averaged regression weights of all conditions, and identified the peak coordinate within the superior IPS adjacent to the gyri crown of the inferior parietal lobe (Fig. 1C). This location was chosen instead of a peak deep within the IPS, which may be less effective targets for tb-TMS. Each subject's peak coordinate was used as our subject-specific TMS target. We chose the right or left IPS depending on which hemisphere showed the strongest effect (right: 13 subjects, left: 4 subjects). Medial S1 was used as the control TMS site, defined anatomically at the most superior portion of the right postcentral gyrus. These analyses were performed within each individual subject's native space but are displayed in MNI space for visualization purposes.

TMS Procedure

TMS was applied via a MagStim Super Rapid 2 stimulator using a figure-eight double air film coil with a 70-mm diameter. For each subject, the TMS intensity for continuous theta-burst stimulation (cTBS) was defined as 80% of the active motor threshold (AMT). Briefly, electromyography was recorded using electrodes from the first dorsal interosseous muscle of the participant's left or right hand depending on the stimulated hemisphere. To determine the AMT, TMS pulses were delivered over the primary motor cortex where TMS produced the largest motor-evoked potential (MEP). AMT was then defined as the minimum TMS intensity required to produce a peak MEP exceeding 50 μV on

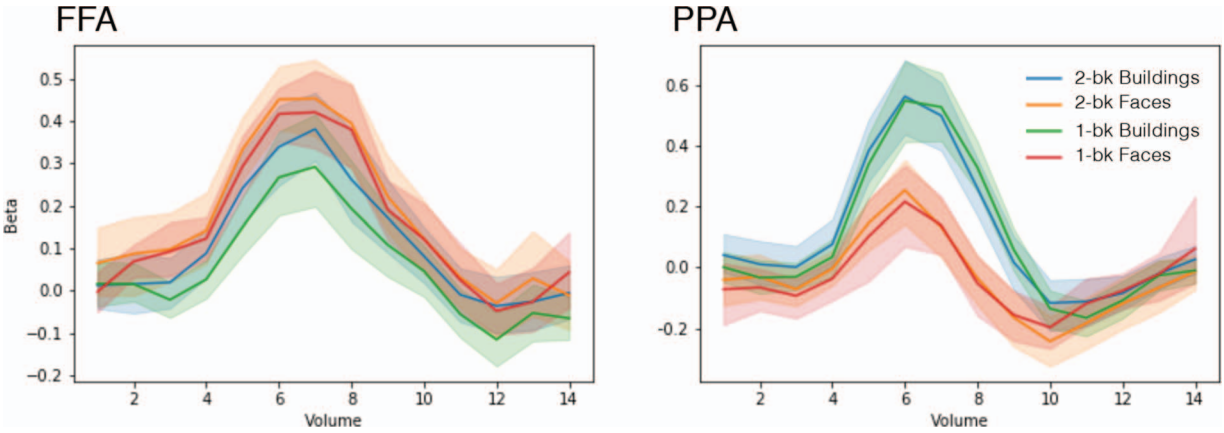

Figure 2. Evoked response patterns in the FFA and PPA. Shaded areas represent bootstrap 95% confidence intervals.

5 out of 10 stimulation pulses. TMS targets were localized using a computerized frameless stereotaxic system (Brainsight, Rogue Research). The cTBS protocol comprises three single pulses separated by 20 ms (50 Hz), and these triplet pulses were repeated every 200 ms (5 Hz) for a duration of 40 s (Huang et al. 2005). A total of 600 pulses were administered. This stimulation protocol has been shown to reduce MEP and BOLD signal up to 1 h and is thought to reduce cortical excitability (Hubl et al. 2008).

Whole-Brain Regression

Whole-brain GLM maps of each individual subject's MTD regressors were submitted to a group analysis contrasting the effects of memory load (2-back vs. 1-back) and stimuli relevance (relevant stimuli category, e.g., VC-FFA connectivity during attend to face condition, vs. irrelevant stimuli category, e.g., VC-PPA connectivity during attend to face condition). Group-level analysis was performed in MNI space with a linear mixed effects model at each voxel, using generalized least squares with a local estimate of random effects variance (AFNI's 3dMEMA). To correct for multiple comparisons, a whole-brain family-wise error correction was performed using Monte Carlo simulation implemented in the 3dClustSim software from AFNI. An updated spatial autocorrelation function option was used to estimate averaged spatial smoothness for Monte Carlo simulation, which has been shown to keep the false positive rate at 5% (Cox et al. 2017). For all group analyses, we report corrected results using the cluster forming threshold of $P < 0.01$ and a cluster size threshold of $P < 0.01$ (corrected cluster size for MTD regressors were 23 contiguous 2 mm^3 voxels).

Statistical Analysis

To test the behavioral relevance of time-varying functional connectivity strength, MTD scores were extracted from volumes of each trial's stimulus onset. Each individual trial's MTD scores were temporally averaged across 15 TRs centered around each stimuli onset, using the windowing procedure described above. These MTD scores were then sorted by correct and incorrect trials, separately for each condition. Paired t-tests were used to test for differences between correct versus incorrect trials. The trial-by-trial MTD scores were also regressed against each trial's reaction time (RT). The area under the curve of each condition's FIR timecourse was calculated as a proxy for evoked response amplitude.

To test the effect of tb-TMS, a three-way, within-subject analysis of variance test (ANOVA) was performed, crossing conditions (1-back vs. 2-back), stimuli categories (faces vs. buildings), and TMS site (IPS vs. S1) as independent variables. Behavioral measures (RT and accuracy), evoked response amplitude, and MTD connectivity estimates (averaged across timepoints within each condition) were used as dependent variables. For each significant main or interaction effect, follow-up post hoc t-tests were performed, controlling for the family wise error rate using the Bonferroni correction.

Results

Behavioral Performance During the Baseline fMRI Session

During the baseline session, subjects had significantly lower accuracy during the 2-back task when compared to the 1-back task (mean accuracy for 2-back attend to faces condition = 0.67, $SD = 0.25$, mean for 1-back attend to faces = 0.85, $SD = 0.2$, contrasting 2-back versus 1-back: $t(22) = 2.44$, $P = 0.026$; mean accuracy for 2-back attend to buildings = 0.65, $SD = 0.33$, mean accuracy for 1-back attend to buildings = 0.88, $SD = 0.18$, contrasting 2-back versus 1-back: $t(22) = 2.75$, $P = 0.014$). Subjects also had significantly slower RTs during the 2-back task when compared to the 1-back task (mean RT for 2-back attend to faces = 0.96 s, $SD = 0.20$ s, mean RT for 1-back faces = 0.87 s, $SD = 0.22$ s, contrasting 2-back versus 1-back: $t(22) = 2.26$, $P = 0.034$; mean RT for 2-back attend to buildings = 0.90 s, $SD = 0.21$ s, mean RT for 1-back attend to buildings = 0.85 s, $SD = 0.2$ s, $t(22) = 1.50$, $P = 0.15$).

Stimulus Evoked Response Patterns During the Baseline fMRI Session

To analyze the amplitude of evoked responses in FFA and PPA, the area under the curve values of FIR estimates across all TRs for each condition were calculated (Fig. 2). A two-factor repeated measure ANOVA was performed with memory load (2-back vs. 1-back) and stimuli relevance (attend to faces vs. attend to buildings) as independent factors, and area under the curve values as dependent values. For both the FFA and PPA, there

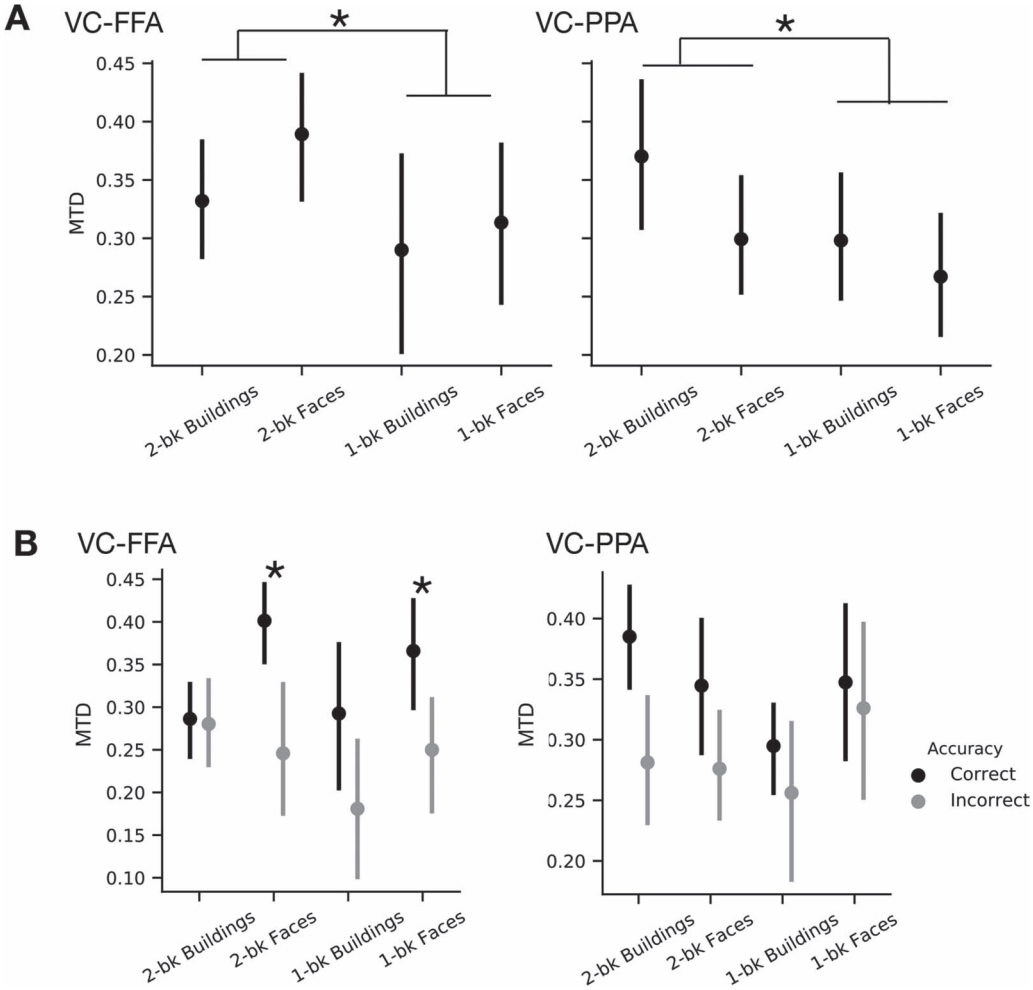

Figure 3. Task-evoked functional connectivity between FFA and VC (VC-FFA), and between PPA and VC (VC-PPA). (*A*) Mean and 95% bootstrap confidence intervals of functional connectivity strength (MTD scores) between VC and FFA/PPA under different experimental conditions. MTD scores were averaged across timepoints within each condition. For both FFA and PPA, functional connectivity strength was significantly modulated by memory load, with PPA further modulated by stimuli relevance. (*B*) Mean and 95% bootstrap confidence intervals of functional connectivity strength (MTD scores) between VC and FFA/PPA for correct and incorrectly performed trials. Functional connectivity strength between VC and FFA were significantly greater for correctly performed trials. MTD scores were extracted the stimulus onset of each trial. Star symbols indicate statistically significant differences between conditions at $P < 0.05$ (corrected).

was an main effect for stimuli relevance (FFA: $F(1,22) = 18.76$, $P < 0.001$; PPA: $F(1,22) = 64.40$, $P < 0.001$). Specifically, evoked response amplitudes were greater during the attend to face conditions in the FFA ($t(22) = 4.33$, corrected $P < 0.001$), and greater during the attend to building conditions in the PPA ($t(22) = 8.03$, corrected $P < 0.001$). These findings replicate our previous study (Hwang et al. 2019). We did not find significant memory load effects for PPA ($F(1,22) = 0.07$, $P = 0.79$). There was a significant memory effect for FFA ($F(1,22) = 5.65$, $P = 0.027$). Specifically, evoked response amplitudes were greater during 2-back attend to face condition compared to the 1-back attend to face condition ($t(22) = 2.38$, corrected $P = 0.027$). No significant memory load by category interactions were found in either the FFA or PPA (FFA: $F(1,22) = 0.66$, $P = 0.43$; PPA: $F(1,22) = 0.47$, $P = 0.5$).

Time-Varying Functional Connectivity During the Baseline fMRI Session

To examine how functional connectivity strength (calculated using time-averaged MTD scores) between VC and FFA/PPA was modulated by stimuli relevance and memory load (2-back vs. 1-back), a repeated measures ANOVA was performed with memory load and stimuli relevance as independent factors, and the time-averaged MTD scores as the dependent variable. We found that functional connectivity between FFA and VC was significantly modulated by memory load (Fig. 3A; $F(1,22) = 6.89$, $P = 0.016$) but not stimuli relevance ($F(1,22) = 2.35$, $P = 0.14$). Post hoc tests showed that compared to the 1-back condition, the 2-back condition elicited stronger functional connectivity between FFA and VC ($t(22) = 2.62$, corrected $P = 0.015$). Functional connectivity between PPA and VC were significantly modulated by both memory load ($F(1,22) = 4.83$, $P = 0.039$) and stimuli relevance ($F(1,22) = 7.81$, $P = 0.011$). Compared to the attend to faces condition, the attend to buildings condition elicited stronger functional connectivity between VC and PPA ($t(22) = 2.79$, corrected $P = 0.011$). Post hoc tests showed that the 2-back condition elicited significantly stronger functional connectivity between PPA and VC when compared to the 1-back condition ($t(22) = 2.2$, corrected $P = 0.039$). These results replicate our previous findings indicating that task-evoked functional

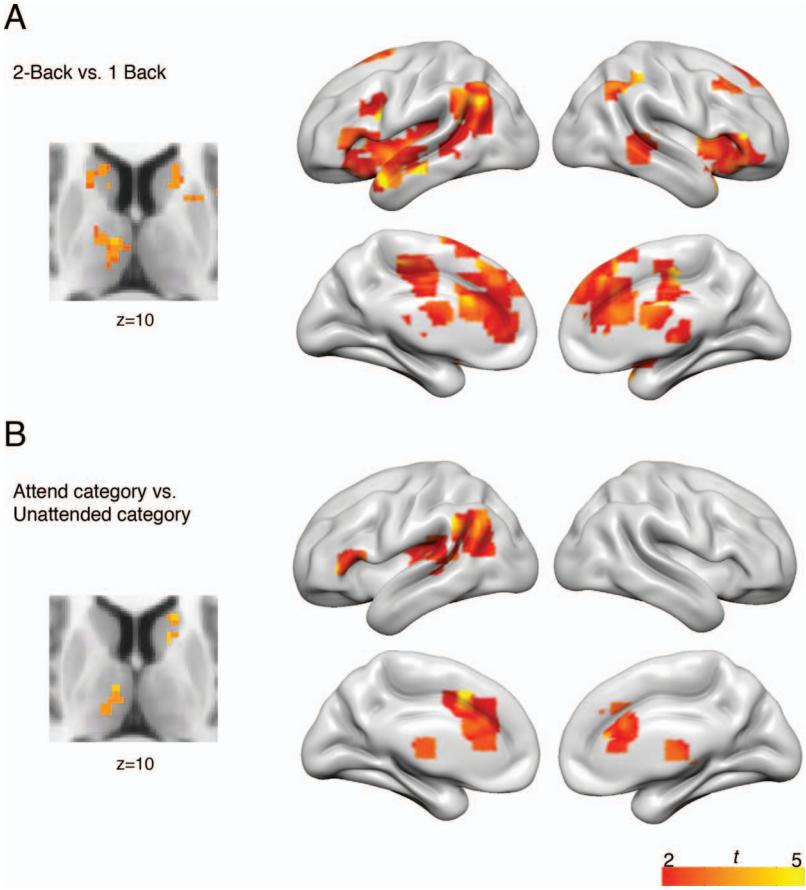

Figure 4. Potential sources of top-down biasing signals that influence functional connectivity patterns during the baseline session. (*A*) Regions that showed significant interactions with task-evoked connectivity patterns associated with increases in memory load (contrasting 2-back vs. 1-back conditions). (*B*) Regions that showed significant interactions with task-evoked connectivity patterns associated with processing of attended stimuli (contrasting the attended stimuli category vs. the unattended category). Both maps were generated using a smoothing window of 15 volumes, cluster corrected at $P < 0.01$.

connectivity between VC and PPA can be enhanced to prioritize building stimuli that are relevant to the task, and further suggest that functional connectivity between VC and FFA/PPA can be further strengthened in response to higher memory load.

To further test the behavioral significance of task-evoked functional connectivity, each trial's MTD score for the time-point of stimuli onset was extracted. The average trial-by-trial MTD scores for correct versus incorrect trials were separately calculated and paired t-tests were performed to test for their differences. We found that functional connectivity between VC and FFA was stronger for correct trials versus incorrect trials during the 2-back attend to face condition (Fig. 3B; $t(22) = 4.97$, corrected $P < 0.001$) and 1-back attend to face condition ($t(22) = 7.98$, corrected $P < 0.001$). No significant differences were found between correct and incorrect trials for connectivity between VC and PPA (2-back condition: $t(22) = 2.18$, corrected $P = 0.08$; 1-back condition: $t(23) = 1.48$, corrected $P = 0.31$).

Relationship between task-evoked time-varying functional connectivity and regional activity

To localize potential regions that modulate task-evoked functional connectivity between VC and FFA/PPA, we entered each condition's time-varying MTD scores as additional regressors into a whole-brain GLM analysis. We first performed whole-brain regressions to identify regions interacting with connectivity patterns that were correlated with increased memory load (Fig. 4A). We found a distributed set of regions that included the right middle frontal gyrus, bilateral inferior frontal gyrus, medial dorsal frontal cortex, bilateral insula, bilateral IPS, left inferior parietal lobule, superior and anterior temporal cortex, bilateral caudate, and the right mediodorsal thalamus. Some of these regions were consistent with our previous study (Hwang et al. 2019), in which we found increased activity in lateral middle frontal, medial frontal, and bilateral IPS associated with changes in connectivity patterns between the 1-back and 0-back tasks. We further contrasted stimuli relevance (e.g., VC-FFA vs. VC-PPA for attend to face conditions, and VC-PPA vs. VC-FFA for attend to building conditions) to localize regions that showed an increased correlation with functional connectivity between regions that support task-relevant information (Fig. 4B). We found increased activity in the left inferior frontal, medial dorsal frontal cortex, left inferior parietal lobule, left superior temporal cortex, left caudate, and the right mediodorsal thalamus.

TMS effects

Our past and current findings demonstrate that among several cortical regions, IPS activity is consistently correlated with

changes in task-evoked functional connectivity between visual areas that process relevant information. However, it is unknown whether IPS is the source of a top-down biasing signal that influences functional connectivity, or whether its activity merely covaries with patterns of functional connectivity but has no active influence over functional connectivity strength. For example, the same patterns may emerge if the IPS is maintaining representation of working memory content through receiving information from task-relevant regions that are functionally coupled. To test these possibilities, we applied tb-TBS to IPS and S1 prior to subjects performing a task during fMRI scanning. To assess TMS effects, we conducted three separate three-way repeated measure ANOVA, using time-averaged MTD scores between VC and FFA/PPA, evoked response amplitude (area under the curve values of FIR estimates), and behavioral data (RT and accuracy) as the dependent measures, and TMS site (IPS vs. S1), memory load, and stimuli relevance as independent factors.

There was no significant difference in trial accuracy following TMS to different sites (main effect of TMS site: $F(1,16) = 2.17$, $P = 0.16$), and no significant interactions between TMS sites and task conditions (TMS site by stimuli relevance interaction: $F(1,16) = 1.65$, $P = 0.22$; TMS site by memory load interaction: $F(1,16) = 0.88$, $P = 0.36$; TMS site by memory load by stimuli relevance: $F(1,16) = 0.51$, $P = 0.48$). There was also no significant difference in RT following TMS to different sites (main effect of TMS site: $F(1,16) = 0.015$, $P = 0.91$), and no significant interactions between TMS sites and task conditions (TMS site by stimuli relevance interaction: $F(1,16) = 1.26$, $P = 0.28$; TMS site by memory load interaction: $F(1,16) = 0.77$, $P = 0.39$; TMS site by memory load by stimuli relevance: $F(1,16) = 0.02$, $P = 0.89$). We further compared trial accuracy and RTs between the baseline session and the S1 tb-TMS session by including whether or not subject received S1 tb-TMS as an independent variable in a separate three-way ANOVA. We found no significant differences in task performances between the baseline session and the S1 tb-TMS session (main effect of TMS on accuracy: $F(1,16) = 1.21$, $P = 0.29$; main effect of TMS on RT: $F(1,16) = 2.18$, $P = 0.17$).

In both the FFA and PPA, there were no significant differences in evoked response amplitudes following TMS to different sites (FFA: main effect of TMS site $F(1,16) = 2.76$, $P = 0.11$; PPA: main effect of TMS site $F(1,16) = 3.20$, $P = 0.09$; Fig. 5A), and there were no significant interactions between TMS site and memory load (FFA: $F(1,16) = 0.005$, $P = 0.94$, PPA: $F(1,16) = 0.08$, $P = 0.77$), nor between TMS site and stimuli relevance (FFA: $F(1,16) = 0.20$, $P = 0.66$, PPA: $(F1,16) = 0.03$, $P = 0.87$). No significant three way interactions between TMS sites, stimuli relevancy, and memory load were found (FFA: $F(1,16) < 0.001$, $P = 0.99$; PPA: $F(1,16) = 1.90$, $P = 0.19$).

For functional connectivity between VC and FFA, there were no significant differences between TMS sites (IPS vs. S1; $F(1,16) = 1.78$, $P = 0.20$; Fig. 5B), and no significant interactions between TMS sites and task factors (TMS site by task relevancy: $F(1,16) = 0.99$, $P = 0.45$; TMS site by memory load: $F(1,16) = 1.42$, $P = 0.25$). However, for functional connectivity between VC and PPA, there was a significant interaction between TMS site and stimuli relevance ($F(1,16) = 16.10$, $P = 0.001$), and between TMS site and memory load ($F(1,16) = 5.18$, $P = 0.037$). Post hoc tests showed that compared to S1 TMS, IPS TMS significantly reduced functional connectivity strength between VC and PPA during the 2-back ($t(16) = 5.04$, corrected $P < 0.001$) and the 1-back attend to building condition ($t(16) = 3.04$, corrected $P = 0.03$). There were no significant differences in other contrasts.

Exploratory analyses

Given that we only observed significant tb-TMS effects on task-evoked functional connectivity between VC and PPA for the 2-back attend to buildings condition, we considered the possibility that brain regions not modulated by tb-TMS may have provided compensatory modulations for other task conditions. Thus, we performed an exploratory analysis to test if after IPS tb-TMS there were brain regions that showed increased association with task-evoked functional connectivity, which could indicate a compensatory response. We first contrasted time-varying connectivity regression maps from all conditions between S1 and IPS tb-TMS sessions. We found that, compared to S1 tb-TMS, the right middle frontal gyrus and the left insula showed increased association with functional connectivity patterns after IPS tb-TMS. In contrast, the stimulated IPS region, the right superior IPS, and its adjacent inferior IPS all showed decreased association with task-evoked functional connectivity (Fig. 6A). Furthermore, given that we did not observe any significant tb-TMS effects on task-evoked functional connectivity between VC and FFA, we performed a second exploratory analysis to probe the possibility that functional connectivity between VC and FFA also received compensatory modulations. We contrasted the VC-FFA connectivity regression maps between IPS and S1 tb-TMS sessions for all attend to face conditions. We found that after IPS tb-TMS, bilateral insula showed increased association with VC-FFA functional connectivity (Fig. 6B). These results suggest that tb-TMS to the IPS disrupted its association with task-evoked functional connectivity, whereas the right MFG and the insula may have provided compensatory modulations over functional connectivity. We also compared VC-FFA and VC-PPA connectivity regression maps, and did not find any significant cluster. We also did not find significant correlations between task performance and TMS effects on functional connectivity, evoked responses, and regression coefficients in regions interacting with functional connectivity.

Discussion

In this study, we investigated how top-down biasing signals influence task-evoked functional connectivity to process task-relevant stimuli, as well as how these signals respond to varying memory load. We found that during an n-back task, functional connectivity between occipital and ventral temporal brain regions that process task-relevant visual stimuli increased as a function of memory load. To search for sources of top-down biasing signals that modulate functional connectivity, we combined time-varying functional connectivity analysis with whole-brain regression. We found several cortical and subcortical regions, including multiple frontal regions, insula, IPS, caudate, and the mediodorsal thalamus, that showed increased covariation with task-evoked changes in functional connectivity. Given the IPS showed strongest effects in our previous study and has been shown to adaptively gate information transfer between visual regions for selective attention (Friston and Buschel 2000; Stephan et al. 2008), we then used tb-TMS to test the causal role of IPS in influencing functional connectivity. We found that tb-TMS to IPS reduced its association with time-varying functional connectivity, and decreased task-evoked modulations in functional connectivity between VC and PPA, specifically during conditions when the PPA was processing task-relevant stimuli. Together, these findings suggest that the human IPS is one source of top-down biasing signals that

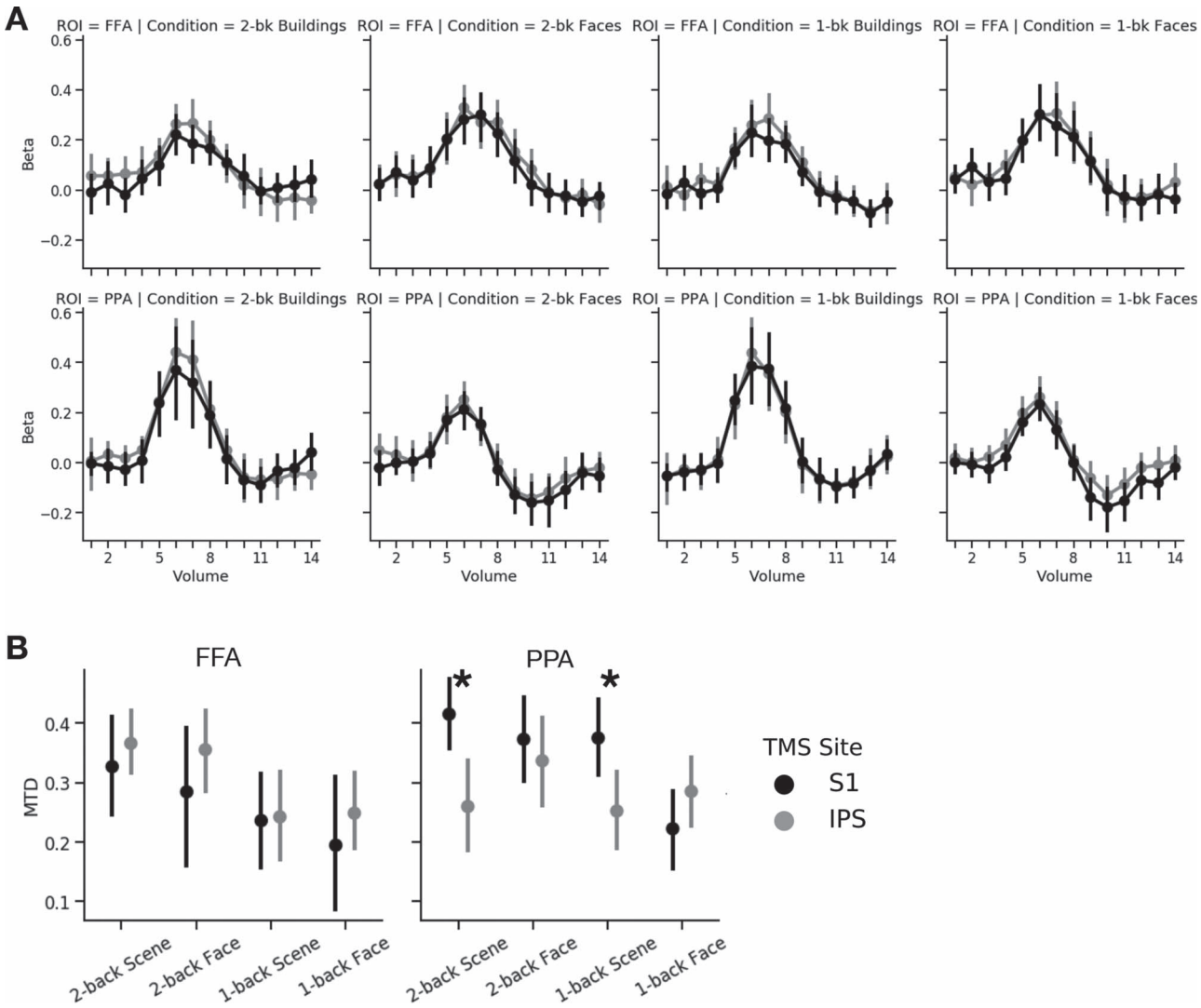

Figure 5. TMS effects on evoked response amplitude and functional connectivity. (*A*) TMS effects on evoked response amplitudes in FFA and PPA for all conditions. Error bars represent 95% confidence intervals. Error bars are 95% bootstrap confidence intervals (*B*) Mean and 95% bootstrap confidence intervals of functional connectivity strength (MTD scores) between VC and FFA/PPA after S1 and IPS TMS. MTD scores were averaged across timepoints within each condition. Star symbols indicate statistically significant differences between conditions at corrected $P < 0.05$.

modulate task-evoked functional connectivity between brain regions that process task-relevant stimuli.

Several theoretical models hypothesize that flexible, goal-directed behaviors are supported by top-down biasing signals that adaptively modulate ongoing sensory, motor, and cognitive processes (Botvinick et al. 2001; Gazzaley and Nobre 2012). Top-down biasing signals are proposed to modulate the response amplitude of localized brain activity to enhance the representation of information that is behaviorally relevant (Desimone 1998; Badre 2008). This model has received extensive empirical support from both non-human primate electrophysiology and human neuroimaging studies (O'Craven et al. 1999; Treue and Trujillo 1999). Our results replicate these previous findings, by demonstrating that stimuli that were relevant to the task elicit stronger stimuli-evoked responses in FFA and PPA.

In addition to the response amplitude modulation mechanism, it was also proposed that information communication between brain regions can be selectively enhanced to prioritize information transfer that is behaviorally relevant (Botvinick et al. 2001; Miller and Cohen 2001). Findings from our current and previous study (Hwang et al. 2019), as well as other previously published studies (Al-Aidroos et al. 2012), support this connectivity modulation mechanism by demonstrating that functional connectivity between VC and FFA or PPA can be selectively enhanced depending on the visual category (faces or buildings) that is task relevant. In our n-back task, we presented face and buildings stimuli that were transparent and overlapping. Therefore, when subjects attended to stimuli from the attended category, stimuli from the other category became irrelevant distractors. Since successful performance requires task-relevant stimuli to be prioritized over task-irrelevant stimuli, representations of the memorized target stimuli must be sustained in absence of external visual stimuli. A connectivity modulation mechanism could prioritize the target over distractors by selectively strengthening the neural pathways that transmit visual features of the attended stimuli

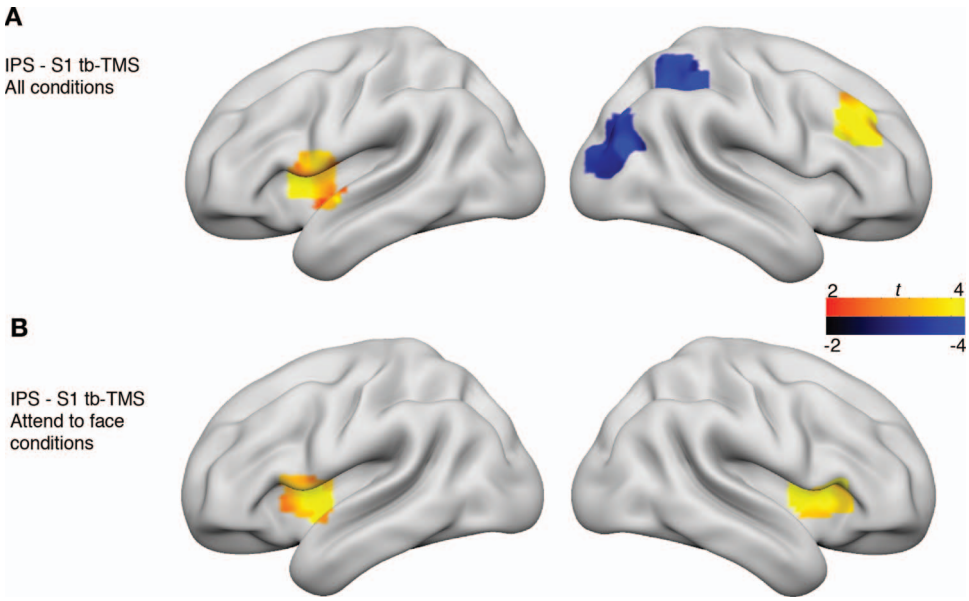

Figure 6. Potential sources of compensatory top-down biasing signals that influence functional connectivity patterns after IPS tb-TMS. (*A*) Contrast of time-varying functional connectivity regression maps between IPS and S1 tb-TMS for all conditions. (*B*) Contrast of VC-FFA time-varying functional connectivity regression maps between IPS and S1 tb-TMS for attend to faces conditions. Yellow color indicates increased association with task-evoked functional connectivity after IPS tb-TMS, and blue color indicates reduced association. No significant cluster were found in medial regions thus not shown. Cluster corrected at $P < 0.01$.

between VC and FFA or PPA, depending on which higher-order visual region encodes the selected visual category. Furthermore, because higher memory load increases the number of visual feature representations that must be maintained in memory, a connectivity modulation mechanism could also actively maintain memory representations by selectively increasing interactions between VC and FFA/PPA. Thus, the increased functional connectivity between the VC and the FFA/PPA observed during comparison of the 2-back condition with the 1-back condition likely reflects increased feedback and feedforward interactions along the ventral stream engaged during higher memory load. If a connectivity modulation mechanism is important for selecting task-relevant stimuli and maintaining memory representation, then the strength of connectivity should be correlated with behavioral performance. Indeed, we found that accurately performed trials had stronger functional connectivity strength between VC and FFA when compared to error trials.

In aggregate, top-down signals can adaptively modulate both localized evoked responses and functional connectivity between task-relevant brain regions to change the signal strength of information depending on its behavioral relevance and task requirement. The prefrontal and parietal cortices have been suggested to be the sources of top-down biasing signals (Miller and D'Esposito 2005; Kay and Yeatman 2017). In support of this notion, both lesion and TMS studies indicate that diminished frontal lobe function causes a reduction in the amplitude of stimulus-evoked responses in posterior brain regions (Knight et al. 1999; Ruff et al. 2008; Higo et al. 2011; Zanto et al. 2011). For example, applying TMS to the frontal eye fields (Heinen et al. 2014), the dorsal lateral prefrontal cortex (Feredoes et al. 2011), the inferior frontal junction (Zanto et al. 2011; Zanto et al. 2013), and the frontal operculum (Higo et al. 2011) have all been shown to modulate evoked responses in downstream cortical regions that process task-relevant stimuli. Previous studies have also found that applying TMS to the motor cortex decreased functional connectivity between the stimulated primary motor area and the anatomically connected putamen (van Schouwenburg et al. 2010). Our findings provide causal evidence indicating that tb-TMS to the IPS modulates functional connectivity between task-related regions not directly stimulated by TMS, and independent of changes in evoked responses. Specifically, we found that tb-TMS to the IPS reduced task-evoked changes in functional connectivity between VC and PPA during conditions when PPA is actively processing task-relevant stimuli. While we found that IPS TMS had an effect on PPA's functional connectivity with VC, it did not alter evoked response amplitudes in either FFA or PPA. Previous studies that reported significant modulations in evoked responses after TMS did not stimulate the IPS (Feredoes et al. 2011; Zanto et al. 2013; Heinen et al. 2014). These results suggest that mechanisms involved in modulating task-evoked response amplitudes could be dissociated from those that influence functional connectivity patterns (Gratton et al. 2016; Gratton et al. 2018), in which case evoked responses and functional connectivity could be modulated by distinct frontal and parietal regions. Altogether, our results demonstrate a role for the IPS in biasing patterns of task-evoked functional connectivity independent of evoked responses.

We found that IPS tb-TMS did not elicit significant changes in behavior. While several previous TMS-fMRI studies also did not find significant changes in behavior after TMS (Feredoes et al. 2011; Zanto et al. 2013), studies that did find significant differences reported TMS modulations in evoked responses (van Schouwenburg et al. 2010; Zanto et al. 2011; Heinen et al. 2014). Therefore, intact task modulations in evoked responses in FFA and PPA may have provided a compensatory mechanism for active maintenance of memory representations and support successful performance. It is also possible that behavioral performance is less sensitive to IPS tb-TMS in our task. Similarly, one potential explanation as to why we found that IPS tb-TMS

did not elicit significant changes in task-evoked functional connectivity between VC and FFA is that other unstimulated brain regions may have provided compensatory top-down modulations. In support of this notion, we found that compared to S1, IPS tb-TMS increased the association between task-evoked functional connectivity and several frontal regions, including the right MFG and the insula. Therefore, it is possible that instead of the IPS, these compensatory regions may have exerted top-down biasing signals to modulate task-evoked functional connectivity in conditions that were not affected by IPS tb-TMS. Two previous TMS-fMRI studies also found evidence that unstimulated regions can provide such a compensatory mechanism (Lee and D'Esposito 2012; Zanto et al. 2013). Finally, it is possible that in our study the FFA and PPA responded differently to a dampened top-down bias signal following TMS to IPS. For example, compared to PPA, several studies have found that evoked responses in FFA consistently exhibit a smaller effect size and weaker task modulation (e.g., Gazzaley et al. 2005; Hwang et al. 2019). Further, a previous fMRI study reported a significant modulation in PPA, but not FFA, following TMS to the right inferior frontal junction (Zanto et al. 2013). Given that task modulations in evoked responses are likely mediated by top-down biasing signals (Gregoriou et al. 2014), both evoked responses and functional connectivity to FFA could be less sensitive to top-down bias signals. A possible explanation for this finding may be related to the fact that building stimuli are capable of driving strong responses in FFA, as indicated by strong evoked responses to building stimuli in our current (see Fig. 2) and previous studies (Gazzaley et al. 2005; Hwang et al. 2019). Thus, FFA's strong response to building stimuli may be causing a mutual inhibition effect that weakens FFA's response to task modulations. This weakened task effect could have masked potential TMS effects in our study.

We previously hypothesized that two potential mechanisms could support the top-down control of information flow between distributed brain regions (Hwang et al. 2019). First, interregional communication may be modulated by regulating the coherence of neural oscillations between brain regions (Fries 2015). Sources of top-down biasing signals could simultaneously target inhibitory neurons that are capable of modulating local neural oscillations in both VC and FFA/PPA (Cardin et al. 2009; Vierling-Claassen et al. 2010), therefore adaptively regulating neural synchrony between task-relevant regions. A second potential mechanism involves the IPS or other frontal regions influencing thalamic activity, potentially the pulvinar nucleus, which in turn modulates connectivity between multiple brain regions through converging cortico-thalamo-cortical connectivity (Saalmann et al. 2012; Sherman 2016). We found that activity in the caudate and the mediodorsal thalamus showed increased associations with task-evoked changes in functional connectivity. Given that the mediodorsal thalamus receives projections from multiple frontal regions and the posterior parietal cortex, but not ventral temporal regions (Selemon and Goldman-Rakic 1988), and that the caudate does not directly project to occipito-temporal regions, the caudate and the mediodorsal thalamus are likely not directly involved in modulating information relay between VC and FFA/PPA. Instead, this cortico-striatal-thalamic loop could be involved in maintaining task-related information in frontal and parietal cortices for top-down control. This hypothesis is supported by a recent study demonstrated that the mediodorsal nucleus is necessary for maintaining task-rule information representation in the frontal cortex (Schmitt et al. 2017).

Funding

National Institutes of Health (NIH) (RO1 MH063901, F32 NS090757); National Science Foundation through their Major Research Instrumentation Program (BCS-0821855).

Notes

We thank Nadia Demilly-Otteson, Kyla Woyshner, Ashton Teng, and Agnes Zhu for assistance in data collection.

References

Al-Aidroos N, Said CP, Turk-Browne NB. 2012. Top-down attention switches coupling between low-level and high-level areas of human visual cortex. *Proc Natl Acad Sci U S A*. 109(36):14675–14680 doi: 10.1073/pnas.1202095109.

Avants BB, Tustison NJ, Wu J, Cook PA, Gee JC. 2011. An open source multivariate framework for n-tissue segmentation with evaluation on public data. *Neuroinformatics*. 9:381–400.

Badre D. 2008. Cognitive control, hierarchy, and the rostro-caudal organization of the frontal lobes. *Trends Cogn Sci*. 12:193–200.

Botvinick MM, Braver TS, Barch DM, Carter CS, Cohen JD. 2001. Conflict monitoring and cognitive control. *Psychol Rev*. 108:624–652.

Cardin JA, Carlén M, Meletis K, Knoblich U, Zhang F, Deisseroth K, Tsai L, Moore CI. 2009. Driving fast-spiking cells induces gamma rhythm and controls sensory responses. *Nature*. 459(7247):663.

Chen AJ, Britton M, Turner GR, Vytlacil J, Thompson TW, D'Esposito M. 2012. Goal-directed attention alters the tuning of object-based representations in extrastriate cortex. *Front Hum Neurosci*. 6:187.

Cole MW, Ito T, Schultz D, Mill R, Chen R, Cocuzza C. 2019. Task activations produce spurious but systematic inflation of task functional connectivity estimates. *NeuroImage*. 189:1–18.

Cox RW, Chen G, Glen DR, Reynolds RC, Taylor PA. 2017. FMRI clustering in AFNI: false-positive rates redux. *Brain Connect*. 7:152–171.

D'Esposito M, Postle BR. 2015. The cognitive neuroscience of working memory. *Annu Rev Psychol*. 66:115–142.

Dale AM, Fischl B, Sereno MI. 1999. Cortical surface-based analysis. I. Segmentation and surface reconstruction. *NeuroImage*. 9:179–194.

Desimone R. 1998. Visual attention mediated by biased competition in extrastriate visual cortex. *Philos Trans R Soc Lond B Biol Sci*. 353:1245–1255.

Destrieux C, Fischl B, Dale A, Halgren E. 2010. Automatic parcellation of human cortical gyri and sulci using standard anatomical nomenclature. *NeuroImage*. 53:1–15.

Druzgal TJ, D'Esposito M. 2001. Activity in fusiform face area modulated as a function of working memory load. *Cognitive Brain Res*. 10:355–364.

Epstein R, Harris A, Stanley D, Kanwisher N. 1999. The parahippocampal place area: recognition, navigation, or encoding. *Neuron*. 23:115–125.

Esteban O, Markiewicz CJ, Blair RW, Moodie CA, Isik AI, Erramuzpe A, Kent JD, Goncalves M, DuPre E, Snyder M. 2019. FMRIPrep: a robust preprocessing pipeline for functional MRI. *Nature methods* 16(1):111.

Feredoes E, Heinen K, Weiskopf N, Ruff C, Driver J. 2011. Causal evidence for frontal involvement in memory target main-

tenance by posterior brain areas during distracter interference of visual working memory. *Proc Natl Acad Sci U S A*. 108:17510–17515.
Fischl B, Sereno MI, Dale AM. 1999. Cortical surface-based analysis. Ii: inflation, flattening, and a surface-based coordinate system. *NeuroImage*. 9:195–207.
Fries P. 2015. Rhythms for cognition: communication through coherence. *Neuron*. 88:220–235.
Friston KJ. 2009. Modalities, modes, and models in functional neuroimaging. *Science*. 326:399–403.
Friston KJ, Buchel C. 2000. Attentional modulation of effective connectivity from V2 to V5/MT in humans. *Proc Natl Acad Sci U S A*. 97(13):7591–7596.
Gazzaley A, Nobre AC. 2012. Top-down modulation: bridging selective attention and working memory. *Trends Cogn Sci*. 16:129–135.
Gazzaley A, Cooney JW, McEvoy K, Knight RT, D'Esposito M. 2005. Top-down enhancement and suppression of the magnitude and speed of neural activity. *J Cogn Neurosci*. 17:507–517.
Gratton C, Laumann TO, Gordon EM, Adeyemo B, Petersen SE. 2016. Evidence for two independent factors that modify brain networks to meet task goals. *Cell Rep*. 17:1276–1288.
Gratton C, Laumann TO, Nielsen AN, Greene DJ, Gordon EM, Gilmore AW, Nelson SM, Coalson RS, Snyder AZ, Schlaggar BL *et al*. 2018. Functional brain networks are dominated by stable group and individual factors, not cognitive or daily variation. *Neuron*. 98(2):439–452.
Gregoriou GG, Rossi AF, Ungerleider LG, Desimone R. 2014. Lesions of prefrontal cortex reduce attentional modulation of neuronal responses and synchrony in V4. *Nat Neurosci*. 17:1003–1011.
Heinen K, Feredoes E, Weiskopf N, Ruff CC, Driver J. 2014. Direct evidence for attention-dependent influences of the frontal eye-fields on feature-responsive visual cortex. *Cereb Cortex*. 24:2815–2821.
Higo T, Mars RB, Boorman ED, Buch ER, Rushworth MF. 2011. Distributed and causal influence of frontal operculum in task control. *Proc Natl Acad Sci U S A*. 108:4230–4235.
Huang YZ, Edwards MJ, Rounis E, Bhatia KP, Rothwell JC. 2005. Theta burst stimulation of the human motor cortex. *Neuron*. 45:201–206.
Hubl D, Nyffeler T, Wurtz P, Chaves S, Pflugshaupt T, Luthi M, Von Wartburg R, Wiest R, Dierks T, Strik WK *et al*. 2008. Time course of blood oxygenation level-dependent signal response after theta burst transcranial magnetic stimulation of the frontal eye field. *Neuroscience*. 151:921–928.
Hwang K, Shine JM, D'Esposito M. 2019. Frontoparietal activity interacts with task-evoked changes in functional connectivity. *Cereb Cortex*. 29:802–813.
Julian JB, Fedorenko E, Webster J, Kanwisher N. 2012. An algorithmic method for functionally defining regions of interest in the ventral visual pathway. *NeuroImage*. 60:2357–2364.
Kanwisher N, McDermott J, Chun MM. 1997. The fusiform face area: a module in human extrastriate cortex specialized for face perception. *J Neurosci*. 17:4302–4311.
Kay KN, Yeatman JD. 2017. Bottom-up and top-down computations in word- and face-selective cortex. *Elife*. 6:e22341.
Knight RT, Staines WR, Swick D, Chao LL. 1999. Prefrontal cortex regulates inhibition and excitation in distributed neural networks. *Acta Psychol (Amst)*. 101:159–178.
Lee TG, D'Esposito M. 2012. The dynamic nature of top-down signals originating from prefrontal cortex: a combined fMRI-TMS study. *J Neurosci*. 32:15458–15466.
Lerner Y, Hendler T, Ben-Bashat D, Harel M, Malach R. 2001. A hierarchical axis of object processing stages in the human visual cortex. *Cereb Cortex*. 11:287–297.
Miller BT, D'Esposito M. 2005. Searching for "the top" in top-down control. *Neuron*. 48:535–538.
Miller EK, Cohen JD. 2001. An integrative theory of prefrontal cortex function. *Annu Rev Neurosci*. 24:167–202.
Nelissen N, Stokes M, Nobre AC, Rushworth MF. 2013. Frontal and parietal cortical interactions with distributed visual representations during selective attention and action selection. *J Neurosci*. 33:16443–16458.
O'Craven KM, Downing PE, Kanwisher N. 1999. Fmri evidence for objects as the units of attentional selection. *Nature*. 401:584–587.
Ruff CC, Bestmann S, Blankenburg F, Bjoertomt O, Josephs O, Weiskopf N, Deichmann R, Driver J. 2008. Distinct causal influences of parietal versus frontal areas on human visual cortex: evidence from concurrent TMS-fMRI. *Cereb Cortex*. 18:817–827.
Saalmann YB, Pinsk MA, Wang L, Li X, Kastner S. 2012. The pulvinar regulates information transmission between cortical areas based on attention demands. *Science*. 337: 753–756.
Schmitt LI, Wimmer RD, Nakajima M, Happ M, Mofakham S, Halassa MM. 2017. Thalamic amplification of cortical connectivity sustains attentional control. *Nature*. 545: 219–223.
van Schouwenburg MR, den Ouden HE, Cools R. 2010. The human basal ganglia modulate frontal-posterior connectivity during attention shifting. *J Neurosci*. 30:9910–9918.
Seidl KN, Peelen MV, Kastner S. 2012. Neural evidence for distracter suppression during visual search in real-world scenes. *J Neurosci*. 32:11812–11819.
Selemon LD, Goldman-Rakic PS. 1988. Common cortical and subcortical targets of the dorsolateral prefrontal and posterior parietal cortices in the rhesus monkey: evidence for a distributed neural network subserving spatially guided behavior. *J Neurosci*. 8:4049–4068.
Serences JT, Saproo S, Scolari M, Ho T, Muftuler LT. 2009. Estimating the influence of attention on population codes in human visual cortex using voxel-based tuning functions. *NeuroImage*. 44:223–231.
Sherman SM. 2016. Thalamus plays a central role in ongoing cortical functioning. *Nat Neurosci*. 16:533–541.
Shine JM, Koyejo O, Bell PT, Gorgolewski KJ, Gilat M, Poldrack RA. 2015. Estimation of dynamic functional connectivity using Multiplication of Temporal Derivatives. *Neuroimage*. 122:399–407 doi: 10.1016/j.neuroimage.2015.07.064.
Stephan KE, Kasper L, Harrison LM, Daunizeau J, den Ouden HE, Breakspear M, Friston KJ. 2008. Nonlinear dynamic causal models for fMRI. *Neuroimage*. 42(2):649–662doi: 10.1016/j.neuroimage.2008.04.262.
Treue S, Trujillo JCM. 1999. Feature-based attention influences motion processing gain in macaque visual cortex. *Nature*. 399:575–579.
Van Essen DC, Anderson CH, Felleman DJ. 1992. Information processing in the primate visual system: an integrated systems perspective. *Science*. 255:419–422.
Vierling-Claassen D, Cardin JA, Moore CI, Jones SR. 2010. Computational modeling of distinct neocortical oscillations driven by cell-type selective optogenetic drive: separable resonant circuits controlled by low-threshold spiking and fast-spiking interneurons. *Front Hum Neurosci*. 4:198.

Visscher KM, Miezin FM, Kelly JE, Buckner RL, Donaldson DI, McAvoy MP, Bhalodia VM, Petersen SE. 2003. Mixed blocked/event-related designs separate transient and sustained activity in fMRI. *NeuroImage*. 19:1694–1708.

Willenbockel V, Sadr J, Fiset D, Horne GO, Gosselin F, Tanaka JW. 2010. Controlling low-level image properties: the SHINE toolbox. *Behav Res Methods*. 42:671–684.

Zanto TP, Chadick JZ, Satris G, Gazzaley A. 2013. Rapid functional reorganization in human cortex following neural perturbation. *J Neurosci*. 33:16268–16274.

Zanto TP, Rubens MT, Thangavel A, Gazzaley A. 2011. Causal role of the prefrontal cortex in top-down modulation of visual processing and working memory. *Nat Neurosci*. 14: 656–661.